Electronic structure and phase stability of $GaAs_{1-x}N_x$ alloys

Jörg Neugebauer and Chris G. Van de Walle
Xerox Palo Alto Research Center, 3333 Coyote Hill Road, Palo Alto, California 94304
(Received 3 November 1994)

Using first-principles total-energy calculations we investigated the electronic structure and stability for several compositions and for various ordered structures of $GaAs_{1-x}N_x$ alloys. Our results show a strong bowing of the band gap which is consistent with recent experimental observations. For certain compositions the alloy may even become metallic; a process which is mainly driven by a strong atomic relaxation. Based on the calculated formation energies and assuming thermodynamic equilibrium a strong miscibility gap between these two structures is found. This is explained in terms of the large mismatch in the lattice constants between GaAs and GaN (more than 20%).

Both GaAs (E_g=1.4 eV) and GaN (E_g=3.5 eV) are important semiconductors for technological applications. The GaAs technology is well established for optoelectronic and high-speed devices; GaN very recently showed a breakthrough in the fabrication of highly efficient blue light emitting diodes.[1] It is interesting to consider from a theoretical point of view whether alloys between GaAs and GaN can be formed, and what their properties would be. The lattice mismatch of more then 20% between GaN and GaAs is larger than for all previously investigated semiconductor alloys.[2,3] Therefore, this system is ideally suited to study the consequences of lattice mismatch on alloy properties such as band-gap bowing, phase stability, and ordering.

For the applications of solid solutions like $GaAs_{1-x}N_x$ it is important to know how the physical properties (electronic band structure, phase stability) change with the composition x. Based on a very simple model, using a quantum dielectric theory, Munich and Pierret predicted a nearly linear monotonic increase in the band gap with increasing composition x.[4] However, recent experimental results by Weyers *et al.* show a strong redshift for small compositions x (x <0.015), indicating an unexpectedly large bowing in the band gap[5] that could even result in a "negative" band gap at large x; the system would be metallic at certain compositions.

In addition to considering the electronic structure, however, one should also address the more fundamental issue of *phase stability*, i.e., whether a solid solution $GaAs_{1-x}N_x$ is thermodynamically stable at all compositions x or whether a *miscibility gap* exists. We have used density-functional theory total-energy calculations to investigate both the electronic structure and the formation energies for several ordered structures in different compositions. An important aspect is atomic relaxation, since GaAs and GaN have a lattice mismatch of more than 20%. Based on the first-principles results and applying a cluster expansion method,[6,7] we derive an approximate phase diagram for the solid solution $GaAs_{1-x}N_x$.

The results presented here were obtained using density-functional theory in the local-density approximation (LDA) for the exchange-correlation functional and soft Troullier-Martins pseudopotentials.[8] The Ga 3d orbitals are treated using the nonlinear core correction.[9] The wave functions are expanded into plane waves up to a cutoff energy of 40 Ry. The k integration over the Brillouin zone is performed on a 4 × 4 × 4 Monkhorst-Pack mesh.[10] Details of the method and convergency checks can be found elsewhere.[11,12]

We start our discussions with zinc blende (111) superlattices having different compositions. Each (111) superlattice has two external degrees of freedom: the lattice constant $a_{\rm lat}$ and the c/a ratio. We define c/a to be unity for bulk zinc blende. In order to obtain the energetically most stable structure, the total-energy of the system was calculated for a mesh of values for $a_{\rm lat}$ and the c/a ratios. At each meshpoint ($a_{\rm lat}$, c/a) all internal parameters (the atomic coordinates) were completely relaxed using the Hellman-Feynmann forces. The resulting total-energy surface is shown in Fig. 1 for the simplest system, the (1+1) GaAs/GaN (111) superlattice. Here, an ($n+m$) superlattice consists of n atomic double layers GaAs and m atomic double layers GaN.

The striking feature in Fig. 1 is that despite the large mismatch of GaAs and GaN the c/a ratio is very close

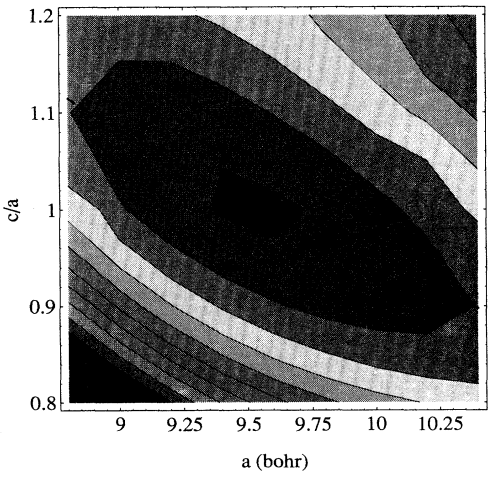

FIG. 1. Contour plot of the total-energy surface for a $GaAs_{0.5}N_{0.5}$ (111) supercell. The contour spacing is 0.5 eV. The dashed line shows the optimum c/a ratio for each lattice constant.

TABLE I. Calculated equilibrium lattice constant a_{lat} and c/a ratio for various compositions x. The numbers in parentheses are for the case where internal relaxation is not allowed.

x	a_{lat} (bohr)	c/a
1/4	9.98	1.02
1/2	9.47	1.01
3/4	8.87 (9.09)	1.00 (1.01)

TABLE II. Bond length after atomic relaxation for the fully relaxed $GaAs_{0.5}N_{0.5}$ (111) supercell. d_1 and d_3 are explained in the text. For bulk GaAs (GaN) $d_1 = d_3 = 4.55$ bohr (3.57 bohr).

Bond	d_1 (bohr)	d_3 (bohr)	d_{bulk} (bohr)
Ga-As	4.49	4.30	4.55
Ga-N	3.57	4.0	3.57

to unity. For the other calculated superlattice structures the tetragonal distortion is also very small (see Table I). Table I lists the equilibrium lattice constant for $GaAs_{1-x}N_x$, with different compositions x: x=0.25 corresponds to a (3+1) GaAs/GaN (111) superlattice and x=0.75 to a (1+3) GaAs/GaN (111) superlattice.

Figure 2 shows that the calculated lattice coordinates for the different structures are in excellent agreement with Vegard's law despite the large lattice mismatch of more than 20%. We note, however, that if internal relaxation is not allowed, significant deviations from Vegard's law occur.

As will be shown in the following discussions a complete relaxation of the atomic structure is essential for a realistic description of the $GaAs_{1-x}N_x$ alloy system. Let us therefore consider the equilibrium atomic structure in more detail. In a (111) superlattice as discussed here, each atom has three symmetrically equivalent neighbors and one additional neighbor. The bond length to the three equivalent neighbors will be called d_3, the bond length to the additional neighbor d_1. Table II displays all the equilibrium bond lengths for the (1+1) GaAs/GaN (111) superlattice. Two features are remarkable: (i) the large difference in d_1 and d_3 for bonds between the same elements (for a Ga–N bond the difference is nearly 0.5 bohr) and (ii) the large strain in the d_3 bonds, whereas the d_1 bonds are close to their bulk value.

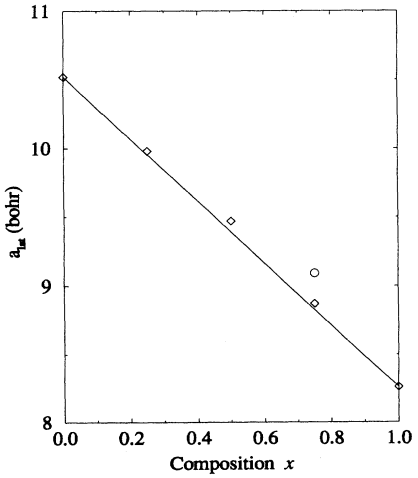

FIG. 2. Comparison of the calculated equilibrium lattice constants (diamonds) with Vegard's law (solid line). The circle shows the equilibrium lattice constant for the case where internal relaxation is not allowed.

From the atomic structure for the relaxed superlattice, shown in Fig. 3, it is evident that d_3^{Ga-As} and d_3^{Ga-N} cannot be chosen independently. Both bond lengths are constrained by the lateral lattice constant: as illustrated in Fig. 3, the projected lengths of both types of d_3 bonds must be equal to $d_{||}$. The lateral lattice constant is adjusted such that the tensile stress in the GaN bonds and the compressive stress in the GaAs bonds is maximally reduced. This is achieved by increasing the angle between the Ga-As bonds and reducing the angle between the Ga-N bonds (Fig. 3). We note that bond bending occurs only to a certain degree. Stronger deviations from the ideal bond angle of 109.47°, which would further reduce the stress in the bonds, are energetically unfavorable; the energy needed for bond bending is clearly not negligible. The limiting mechanism is the rehybridization of the bonds due to bond bending, which would eventually weaken the bonds.

Based on the calculated equilibrium geometry, we computed the band structure for the different superlattices. Figure 4(a), which shows the band structure for a (1+1) GaAs/GaN (111) superlattice, reveals the unexpected fact that the superlattice is metallic. From this result we cannot directly conclude that such a superlattice would indeed be metallic, since the local-density approximation results in an underestimation of the band gap. However, quasiparticle calculations by Rubio and Cohen[13] show a correction for the unrelaxed (1+1) superlattice of ≈ 0.6 eV, which would be too small to open the band gap. In order to understand better the origin of this

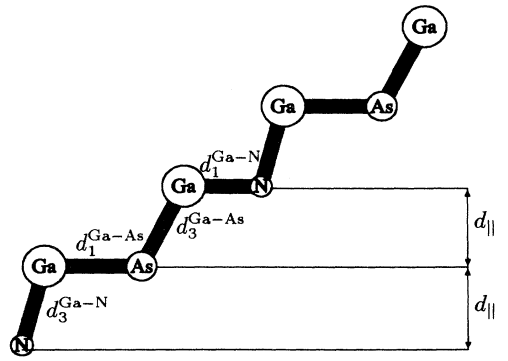

FIG. 3. Atomic structure of the completely relaxed (1+1) GaAs/GaN (111) superlattice along the chains of the (110) plane. The angle between the Ga-N bonds is 105° (113.5°) and between the Ga-As bonds 116.8° (101.2°). The first value is the angle in the plane, the value in parentheses the angle between the back bonds. The lateral spacing is $d_{||}$=3.88 bohr.

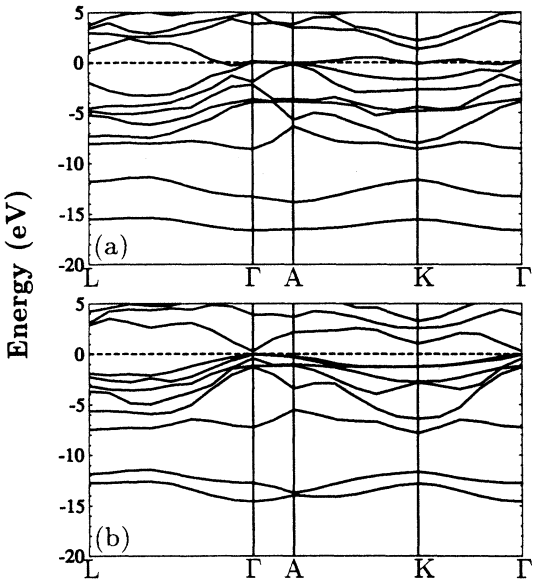

FIG. 4. Band structure for a fully relaxed (a) and nonrelaxed (b) (1+1) GaAs/GaN (111) superlattice. The dashed line marks the Fermi level (a) and the top of the valence band (b). For both band structures the equilibrium values for $a_{\rm lat}$ and c/a as calculated for the relaxed structure were used.

unusual gap closing, we also calculated the band structure for the unrelaxed (1+1) superlattice (see Fig. 4). For this structure we find a band gap of about 0.2 eV, in good agreement with Ref. 13. The qualitative change from a semiconducting superlattice to a metallic superlattice, due to atomic relaxation, emphasizes the importance of the atomic structure for alloys of compounds with strong lattice mismatch and explains the failing of simple approximations, such as the virtual-crystal approximation for this class of alloys.[4] We find that also the (1+3) and the (3+1) GaAs/GaN (111) superlattices are metallic within LDA.

Assuming a parabolic dependence the composition dependent band gap can be written as

$$E_g(x) = E_g^{\rm GaAs}(1-x) + E_g^{\rm GaN}x - bx(1-x) \quad , \qquad (1)$$

where b is the "optical bowing parameter."[14] The experimental measurements of E_g in Ref. 5 were only carried out for $x < 0.015$, and extrapolating may, therefore, be dangerous. Still, using the experimentally measured value of $E_g \approx E_g^{\rm GaAs} - 12\ {\rm eV} \times x$ for $x < 0.015$[5] and the experimentally known band gaps one gets $b \approx -14$ eV. This would result in a closing of the band gap for $0.16 < x < 0.71$, i.e., also the experimental results indicate that solid solutions may become metallic for certain stoichiometries.

The question remains, however, whether and under which conditions these structures are thermodynamically stable. Instead of deriving a complete phase diagram[2] we will estimate an upper limit for the miscibility of GaAs and GaN. Since our results will show that under typical growth conditions the solubility is only a few percent, even a change by a factor of 2 would not alter the conclusion that both components have very limited miscibility.

We define the excess enthalpy as

$$\Delta H(x,s) = E_{\rm tot}^s - xE_{\rm tot}^{\rm GaN} - (1-x)E_{\rm tot}^{\rm GaAs} \qquad (2)$$

for a specific ordered structure s of a $GaAs_{1-x}N_x$ alloy.[2] $E_{\rm tot}^s$ is the total energy per atom for the alloy structure s and $E_{\rm tot}^{\rm GaN}$ ($E_{\rm tot}^{\rm GaAs}$) are the total energies for GaN (GaAs).

Table III lists the calculated excess enthalpies for a variety of different structures, which were chosen to be a minimal basis set for a cluster expansion.[2] We note that the sequence of energies for the different modifications (see Table III),

$$\Delta H(F) < \Delta H(L), \quad x = 0.25 \quad \text{or} \quad x = 0.75 \qquad (3a)$$

$$\Delta H({\rm CH}) < \Delta H({\rm CA}), \quad x = 0.5 \qquad (3b)$$

is the same as found in previous calculations for lattice-mismatched systems.[2,15] We use the calculated excess enthalpies to construct a lower limit $\Delta H^{\rm min}(x)$ for each composition. Figure 5 shows that

$$\Delta H(x,s) < \Delta H^{\rm min}(x) = 4x(1-x)\Delta H^0, \qquad (4)$$

with $\Delta H^0 = 199$ meV is a lower limit for all calculated excess enthalpies. Using this ansatz we can analytically estimate the miscibility gap. The entropy is estimated within a mean-field approximation, which gives an upper limit:

$$S(x) = -k_B[x\ln x + (1-x)\ln(1-x)] \qquad (5)$$

where k_B is the Boltzman constant. The free energy becomes

$$F(x,T) = \Delta H^{\rm min}(x) - TS(x) \quad . \qquad (6)$$

The miscibility gap as a function of temperature is then given by the binodal line[7]

$$k_BT/\Delta H^0 = (8x-4)/[\ln x - \ln(1-x)] \qquad (7)$$

TABLE III. Excess formation enthalpy ΔH according to Eq. (2) and relaxation energy $\Delta E^{\rm rel}$ for different structures and compositions. Symbols for the different structures were taken from Ref. 2.

Structure		x	ΔH (meV/atom)	$\Delta E^{\rm rel}$ (meV/atom)
Luzonite	$L1$	0.25	346	212
Famatinite	$F1$	0.25	149	310
(111) superl. (1+3)	SL	0.25	302	
Chalcopyrite	CH	0.5	227	581
(100) superl. (1+1)	CA	0.5	480	411
(111) superl. (1+1)	SL	0.5	452	
Luzonite	$L3$	0.75	430	391
Famatinite	$F3$	0.75	280	472
(111) superl. (3+1)	SL	0.75	348	

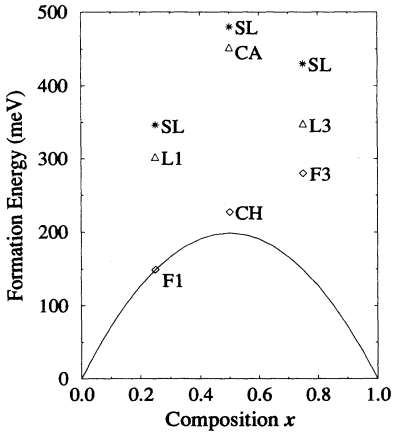

FIG. 5. Excess formation enthalpies for different structures and compositions of ordered $GaAs_{1-x}N_x$. The parabola (solid line) $\Delta H^{\min}(x) = 4x(1-x)\Delta H^0$ with $\Delta H^0 = 4/3 \times \Delta H(\mathrm{F1}) = 199\,\mathrm{meV}$ is a lower limit for all calculated formation enthalpies.

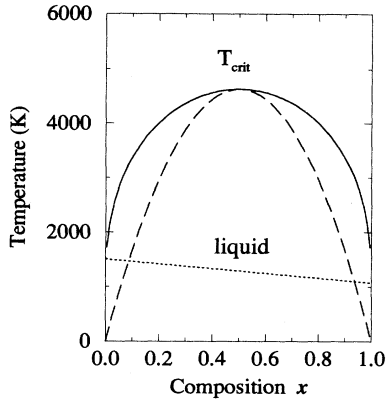

FIG. 6. Lower limit of the miscibility gap (binodal line, solid curve) and spinodal line (dashed curve) for $GaAs_{1-x}N_x$ alloys. The liquidus line (dotted curve) separates the liquid from the solid phase.

and shown in Fig. 6. The critical temperature, above which complete miscibility is possible, is $T_{\mathrm{crit}} = 2\Delta H^0/k_B \approx 4611\,\mathrm{K}$. At typical growth temperatures of $\approx 800\,\mathrm{K}$, we find a solubility limit of less than 2%. This value is consistent with recent experimental results where the authors could achieve a solubility of 1.6% N in GaAs.[5]

Our estimated value for the solubility limit is based on two main assumptions: (i) thermodynamic equilibrium and (ii) the calculated excess enthalpies being a lower limit for all possible structures. Regarding (i), one might expect to improve miscibility by working far away from thermodynamic equilibrium.

The second issue (ii) is related to the question of whether other structures could be energetically more favorable. As shown by Ferreira *et al.*[2] the structures investigated here are a representative basis for all zinc blende structures in the sense that they contain all possible short-range interactions. In particular, our calculated excess enthalpies show that all superlattice structures in the (111) or (100) direction are energetically less stable than a chalcopyrite or famatinite structure, where the strain is maximally relieved by intermixing.

In summary, we have investigated the electronic structure and phase stability of $GaAs_{1-x}N_x$ alloys using first-principles calculations. The most striking features we find for this system are a strong bowing of the band gap and a very limited miscibility. Both features are attributed to the large mismatch (more than 20%) in the lattice constants of GaAs and GaN. We, therefore, expect a similar behavior for other nitrogen-based alloy systems, where the "small" nitrogen atom (r^{N}=0.75) is substituted by much larger anions such as for $InAs_{1-x}N_x$ (r^{As}=1.20) and to a lesser extent for $InP_{1-x}N_x$ (r^{P}=1.06). Both the large bowing of the electronic band gap and the limited miscibility of $GaAs_{1-x}N_x$ alloys are important characteristics of this system.

This work was supported in part by the DAAD (German Academic Exchange Service) and by the AFOSR.

[1] S. Nakamura, T. Mukai, and M. Senoh, Appl. Phys. Lett. **64**, 1687 (1994).
[2] L. G. Ferreira, S.-H. Wei, and A. Zunger, Phys. Rev. B **40**, 3197 (1989).
[3] N. Marzari, S. de Gironcoli, and S. Baroni, Phys. Rev. Lett. **72**, 4001 (1994).
[4] D. P. Munich and R. F. Pierret, Solid-State Electron. **30**, 901 (1987).
[5] M. Weyers, M. Sato, and H. Ando, Jpn. J. Appl. Phys. **31**, L853 (1992).
[6] J. W. D. Conolly and A. R. Williams, Phys. Rev. B **27**, 5169 (1983).
[7] W. R. L. Lambrecht and B. Segall, Phys. Rev. B **47**, 9289 (1993).
[8] N. Troullier and J. L. Martins, Phys. Rev. B **43**, 1993 (1991).
[9] S. G. Louie, S. Froyen, and M. L. Cohen, Phys. Rev. B **26**, 1738 (1982).
[10] H. J. Monkhorst and J. D. Pack, Phys. Rev. B **13**, 5188 (1976).
[11] J. Neugebauer and C. G. Van de Walle (unpublished).
[12] R. Stumpf and M. Scheffler, Comput. Phys. Commun. **79**, 447 (1994).
[13] A. Rubio and M. L. Cohen (unpublished).
[14] J. E. Bernard and A. Zunger, Phys. Rev. B **36**, 3199 (1987).
[15] J. E. Bernard, L. G. Ferreira, S.-H. Wei, and A. Zunger, Phys. Rev. B **38**, 6338 (1988).

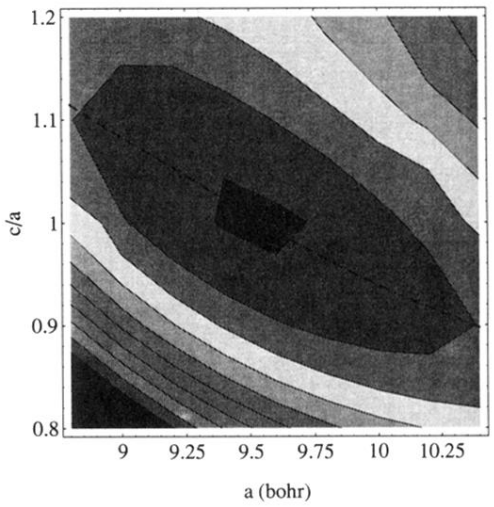

FIG. 1. Contour plot of the total-energy surface for a $GaAs_{0.5}N_{0.5}$ (111) supercell. The contour spacing is 0.5 eV. The dashed line shows the optimum c/a ratio for each lattice constant.